Published in final edited form as:
Neuroimage. 2010 February 15; 49(4): 3436. doi:10.1016/j.neuroimage.2009.11.019.

Executive control function, brain activation and white matter hyperintensities in older adults

Vijay K. Venkatraman, M.S[a], **Howard Aizenstein, M.D, Ph.D**[a,b,*], **Jack Guralnik, MD, PhD**[c], **Anne B. Newman, MD, MPH**[d], **Nancy W. Glynn, PhD**[d], **Christopher Taylor, B.S**[d], **Stephanie Studenski, MD, MPH**[e], **Lenore Launer, PhD**[c], **Marco Pahor, MD**[f], **Jeff Williamson, MD**[g], and **Caterina Rosano, MD, MPH**[d]

[a]Department of Bioengineering, School of Engineering, University of Pittsburgh, 749 Benedum Hall, Pittsburgh, PA, 15261

[b]Department of Psychiatry, University of Pittsburgh, 3811 O'Hara Street, Pittsburgh, PA 15213

[c]National Institute on Aging, Laboratory of Epidemiology, Demography, and Biometry, NIH, 7201 Wisconsin Avenue, Bethesda, MD 20892-9205

[d]Department of Epidemiology, Graduate School of Public Health, University of Pittsburgh, 130 N. Bellefield Avenue, Pittsburgh, PA, 15213

[e]Division of Geriatric Medicine, Department of Medicine, University of Pittsburgh, 3471 Fifth Ave, Kaufmann Medical Building, Suite 500, Pittsburgh, PA 15213

[f]Department of Aging and Geriatric Research, University of Florida - Institute on Aging, 1329 SW 16th Street, Room 5263, PO Box 100107, Gainesville, FL, 32611

[g]Department of Internal Medicine, Section on Gerontology and Geriatric Medicine, Wake Forest University, Medicial Center Boulevard, Winston-Salem, NC 27157

Abstract

Context—Older adults responding to executive control function (ECF) tasks show greater brain activation on functional MRI (fMRI). It is not clear whether greater fMRI activation indicates a strategy to compensate for underlying brain structural abnormalities while maintaining higher performance.

Objective—To identify the patterns of fMRI activation in relationship with ECF performance and with brain structural abnormalities.

Design—Cross-sectional analysis. Main variables of interest: fMRI activation, accuracy while performing an ECF task (Digit Symbol Substitution Test), volume of white matter hyperintensities and of total brain atrophy.

Setting—Cohort of community-dwelling older adults.

Participants—Data were obtained on 25 older adults (20 women, 81 years mean age).

***Corresponding author:** Howard Aizenstein, MD, PhD, GPN Lab, WPIC/UPMC, 3811 O'Hara Street, Pittsburgh, PA 15213, Phone: 412-383-5452, aizen@pitt.edu.

Outcome Measure—Accuracy (number of correct response / total number of responses) while performing the Digit Symbol Substitution Test.

Results—Greater accuracy was significantly associated with greater peak fMRI activation, from ECF regions, including left middle frontal gyrus and right posterior parietal cortex. Greater WMH was associated with lower activation within accuracy-related regions. The interaction of accuracy by white matter hyperintensities volume was significant within the left posterior parietal region. Specifically, the correlation of white matter hyperintensities volume with fMRI activation varied as a function of accuracy and it was positive for greater accuracy. Associations with brain atrophy were not significant.

Conclusions—Recruitment of additional areas and overall greater brain activation in older adults is associated with higher performance. Posterior parietal activation may be particularly important to maintain higher accuracy in the presence of underlying brain connectivity structural abnormalities.

INTRODUCTION

Functional neuroimaging studies of executive control function (ECF) have shown that older adults have greater brain activation within the fronto-parietal regions and also activate additional regions compared to younger adults (Calautti, Serrati et al. 2001; Mattay, Fera et al. 2002; Ward and Frackowiak 2003; Persson, Sylvester et al. 2004; Heuninckx, Wenderoth et al. 2005; Rosano, Aizenstein et al. 2005). This increased activation in the aging brain is well documented for various processes (Cabeza 2002; Reuter-Lorenz and Lustig 2005) including motor control (Mattay, Fera et al. 2002; Ward and Frackowiak 2003) and working memory (Cabeza, Daselaar et al. 2004). Despite previous substantial work, (McIntosh, Sekuler et al. 1999; Reuter-Lorenz, Jonides et al. 2000; Reuter-Lorenz 2001; Rypma 2001; Cabeza, Anderson et al. 2002; Grady 2002; Cabeza, Daselaar et al. 2004; Reuter-Lorenz and Lustig 2005; Park and Reuter-Lorenz 2009) it is not clear whether increased brain activation in older adults is a response to underlying age-related brain structural abnormalities and whether it is important to maintain higher performance.

Previous neuroimaging studies indicate that greater brain activation occurs when there is an imbalance between the difficulty of the task and the neural/ behavioral resources of the individual. For example, young adults have greater brain activation in response to tasks of greater difficulty. (Grady 1996; Rypma and D'Esposito 1999) Similarly, work done by us (Rosano, Aizenstein et al. 2005) and others, (Langenecker, Nielson et al. 2004; Persson, Sylvester et al. 2004) indicate that older adults performing ECF tasks sometimes have greater brain activation compared to younger adults. The decline of neural resources with age can be detected on brain structural MRI as white matter hyperintensities and greater atrophy. Such brain structural abnormalities may be responsible for the patterns of neural activation observed during performance of ECF tasks in older adults. In the presence of such impairments, the brain may respond to the task either with greater activation within ECF-related fronto-parietal regions or more “diffuse” activation with recruitment of non-ECF regions, or both. However, it is not known whether these changes in brain structure and activation are associated with better or worse ECF performance. If greater brain activation in individuals with brain structural impairment is associated with greater accuracy, then this would indicate that older adults’ brain activation may be a compensatory strategy to maintain performance.

With the exception of a few studies of memory (Persson 2006; Persson 2006), previous reports of ECF-related activation could not answer this question because they did not examine the relationship of brain activation with behavioral performance concurrently with brain MRI abnormalities. Studies examining each of these associations individually report that greater fMRI activation in older adults is associated with better performance(Reuter-Lorenz 1999; Cabeza, Anderson et al. 2002; Langenecker, Nielson et al. 2004; Rosano, Aizenstein et al.

2005), while greater brain MRI structural abnormalities are associated with poorer cognitive function (West 1996; Gunning-Dixon and Raz 2000). Recently, a few studies have begun to examine the interaction of fMRI brain activation with structural abnormalities,(Nordahl 2006; Brassen 2009) but did not account for performance.

The objective of this work is to determine whether brain activation in older adults with brain structural impairment is associated with better performance on an ECF task. We will examine fMRI patterns of activation in the whole brain to assess whether greater activation is localized within ECF-related regions or it extends to recruit additional non-ECF regions or both.

METHODS

Participants

Participants for this study were recruited from a larger group of older adults, who had completed a 1-yr physical activity randomized controlled trial LIFE-P (Lifestyle Interventions and Independence For Elders-Pilot) (Pahor, Blair et al. 2006) (www.ClinicalTrials.gov, registration # NCT00116194). The design of the LIFE-P has been described in detail elsewhere (Pahor, Blair et al. 2006). The primary mode of exercise for the intervention group was walking for at least 150 minutes/ week and the active comparison group attended education sessions on nutrition, medications, foot care, and recommended preventive services at different ages. Group assignment to the intervention or active control was treated as a covariate in all analyses.

LIFE-P participants were screened for interest in participating in this brain fMRI study during their follow-up phone call 1.7 years ± 1.7 month after the close-out of the Intervention study. MR eligibility was assessed by self-report and review of medical records. Participants were eligible if they had no history of metallic fragments, cardiac pacemaker, aneurysm clip, cochlear implants, weight of more than 250 lb or claustrophobia. Those who had been hospitalized and/or had surgery in the month prior to the MRI were also excluded. The University of Pittsburgh Institutional Review Board approved the study and all subjects gave written informed consent. A total of 30 participants (mean age: 81.16 years, standard deviation: 3.55 years) were MRI eligible, agreed to participate and received a brain MRI and an in-person exam. These had similar characteristics ($p>0.14$ for all comparisons) compared to the rest of the group interviewed (n=74) with the exception of race (blacks: 10 vs. 37% in the fMRI vs. not fMRI group, Fisher exact test: $p=0.004$).

fMRI Paradigm

The Digit symbol substitution test (DSST) is a test of psychomotor performance, which requires incidental memory, perceptual organization, visuomotor coordination, and selective attention to filter out irrelevant information (e.g., symbols that may look alike) and to perform successfully. (Salthouse 1978; Weschler Adult Intelligence Scale-Revised. San Antonio 1981). The test has high test–retest reliability (Matarazzo and Herman 1984; Salthouse 1996). The DSST is particularly sensitive to cognitive changes associated with aging, (Salthouse 1978; Weschler Adult Intelligence Scale-Revised.San Antonio 1981) especially working-memory, information processing speed and executive control function. In addition to the computerized version of the Salthouse DSST (sDSST) performed during fMRI, participants also performed the pencil and paper version of the DSST, frequently employed in epidemiological studies of older adults.(Rosano, Newman et al. 2008)

sDSST task parameters during fMRI acquisition—The computerized version of the sDSST has been validated by Salthouse (Salthouse 1978; Matarazzo and Herman 1984; Salthouse 1996). In this study, the sDSST was adapted for the fMRI scanning procedure (Figure 1) to test the working memory domain. As illustrated in Figure 1, the subject sees on a computer

screen one number-symbol matching pair (cue). After the cue disappears, an answer key (probe) appears containing a grid of four number-symbol matching pairs. The subject is instructed to push the right- finger button if the probe contains one number-symbol that matches the cue, and to push the left-index finger button if the probe does not contain any number-symbol that matches the cue. Instructions are to respond "as fast as you possibly can". Accuracy and response time during the task were obtained. Accuracy was computed as number of correct responses/ total number of responses. Response time was computed as the interval of time between appearance of the probe and the subject's response. Overall, this version of the DSST can be viewed as a working memory task with one item as the cue and four items as the probe . Thus, unlike the standard DSST, which uses RT as the primary outcome measure, we have chosen in this case to use accuracy, which is often the primary outcome measure for working memory tasks

Participants were instructed on the task outside the magnet for as long as needed to familiarize them with the task (usually 5–10 minutes). The sDSST was presented using a block-design with 8 trials/block, in which a block of the experimental sDSST condition is alternated with control condition for a total of 10 blocks (Figure 1). Each block lasted for 56 secs including 8 secs of instructions at the start of each block to remind the subjects of the task. The 8 seconds of instruction and the first trial of each block were excluded from the analyses (see 'fMRI data analyses' below). The different task conditions (matching vs. non-matching) were randomized 1:1 across the block. The task consisted of a total of 5 sDSST-blocks alternated with 5 control-blocks for a total of 9 minutes and 20 seconds. The control condition was designed to account for the non task-specific brain activation (frontal eye field and visual cortex for eye movements, and motor cortex for the index fingers movements) that are likely to be elicited during sDSST performance in addition to the task-specific activation of the executive control function network. Responses occurring after the probe disappeared (after 3.6 sec) were termed as "no response" and were omitted from the calculation of accuracy and response time. In additional sensitivity analyses the "no response" were coded as "wrong" and with a response time of 3.6 seconds and were thus included in the computation of accuracy and response time.

Functional and Structural MRI

Scanning protocol—The magnetic resonance (MR) images were acquired on a 3 T Siemens Trio MR scanner, using a Siemens 12- channel head coil. Functional MR images were acquired as whole-brain gradient-echo echoplanar images (EPIs) [repetition time (TR), 2 secs; echo time (TE), 32 ms; resolution, 128*128; slice thickness, 3.0 mm; 29 axial slices; GRAPPA with acceleration factor of 2]. Each scanning session started with the acquisition of a three-dimensional MPRAGE high-resolution T1-weighted image (TR, 2.3 secs; TE, 3.43 ms; slice thickness, 1 mm; 176 slices) for anatomical detail (gray matter measure, brain volume and atrophy) and FLAIR T2-weighted image (TR=9 secs; TE= 102 ms; TI= 2.5 secs; slice thickness, 3 mm; 49 slices) for extracting the WMH burden.

Structural brain image analysis—Total volumes of gray matter, white matter, and cerebrospinal fluid were obtained using a previously validated procedure, the Automated Labeling Pathway.(Rosano, Becker et al. 2005; Wu, Carmichael et al. 2006) The Automated Labeling Pathway applies a nonlinear registration algorithm (a fully deformable automatic algorithm) to transform a template brain (the Montreal Neurological Institute Colin27 template) into the native anatomical space of each individual's brain. Total gray matter volume, white matter volume, and cerebrospinal fluid volume were estimated in cubic millimeter by summing all voxels classified as these tissue types. Atrophy index was calculated as the ratio of cerebrospinal fluid volume and gray matter volume. White matter hyperintensity (WMH) volume was obtained using an automated method previously published;(Udupa 1996) and it was normalized for brain volume.

fMRI data processing—Functional imaging data were analyzed with Statistical Parametric Mapping 5 (SPM5)(Friston 1995) (Wellcome Department of Imaging Neuroscience, London, UK) implemented in MatLab (MathWorks, Natick, MA). For each subject, all EPI volumes were realigned to the first volume of the time series, and a mean image of the realigned volumes was created. Standard SPM high pass filter was applied to address low-frequency scanner drift that could potentially contaminate the signal. The realigned images were co-registered to the anatomical T1-weighted image. To normalize the anatomical image as well as the EPIs to a standard SPM reference system the following procedure was applied. First, the anatomical image as well as a representative template image [Montreal Neurological Institute (MNI)] was segmented into gray matter, white matter, and CSF. Then, the anatomical gray matter image was normalized to the gray matter of the MNI brain. Subsequently, the derived normalization parameters were applied to the EPIs, which were subsampled to a voxel size of 2 * 2 * 3 mm and smoothed with a Gaussian kernel of 8 mm FWHM.

Analyses—All analyses were adjusted for group assignment. Participants' characteristics were compared using non-parametric tests. Mann-Whitney test and Fisher exact tests were used to compare differences in means and proportion between groups for continuous and categorical variables, respectively. Non-parametric correlation coefficients were computed to test the association of atrophy index and WMH volume with accuracy. Based on sample size computations for fMRI BOLD signal, (Zandbelt, Gladwin et al. 2008) this study had adequate power of 80% to detect an effect size of at least 0.72 or a significant mean change difference of 0.18% with power alpha =0.05 with a sample size of n=25.

fMRI data analysis—Analyses were performed in the context of the general linear model (Friston 1995). Each condition was modeled using a delayed boxcar function. Block length was of 42 seconds, after excluding the first 8 seconds (instructions) and the first trial. The first trial was excluded to address variability in the hemodynamic response, because in a block design the hemodynamic activity is expected to saturate after the initial hemodynamic up-swing, which should occur by the end of the first trial. Additionally, movement parameters derived from realignment were added as covariates of no interest to correct for confounding effects induced by head movement. Two contrasts of interest were used: sDSST > Control condition and Control condition > sDSST. These were first estimated for each subject individually (averaging activation across runs) and then subjected to a second-level random-effects analysis. For all analyses, the t values were thresholded at a minimal voxel entry value of $T > 1.71$ ($p < 0.05$ uncorrected) and then corrected for multiple comparison using AlphaSim (gray matter mask, 1000 Monte Carlo simulation and smoothness obtained using 3dFWHMx) (Cox 1996) . In all analyses, the clusters with cluster probability (alpha) of 0.001 (extent threshold: 433 voxels) were accepted and identified using WFU_Pickatlas.(Maldjian, Laurienti et al. 2003). Identification was done with WFU_Pickatlas.(Maldjian, Laurienti et al. 2003)

sDSST- related brain fMRI activation and relationship with accuracy—The second-level analyses were performed over all subjects to obtain the two contrasts of interest (sDSST > Control condition and Control condition > sDSST), which were modeled using a one-sample t-test, adjusted for group assignment and atrophy index. The mean group activation maps were estimated at each voxel and restricted to gray matter. Subsequently, the association of fMRI mean signal with accuracy (continuous measure) adjusted for group assignment, sDSST response time and atrophy index was estimated. The activation map was obtained for positively and negatively correlated regions with accuracy.

Relationship of fMRI activation, accuracy and brain structural abnormalities—In subsequent analyses, we tested the associations of WMH volume (or atrophy index) with the mean group activation maps obtained from the sDSST > control condition contrast.

Associations were estimated for each voxel and restricted to gray matter. To investigate the interrelationship between brain structure, brain activation and performance; we also examined the fMRI patterns of interaction of accuracy by WMH volume. Specifically, the model included terms for accuracy, WMH and accuracy * WMH (interaction term). The analyses was adjusted for group assignment, atrophy index and sDSST response time. In additional exploratory analyses we further examined the association of accuracy with fMRI activation among those with WMH measure above the median.

Results

Of the thirty participants who received a brain fMRI, two were excluded from this analysis due to incomplete behavioral data and three were excluded for excessive motion artifacts (±3.5 mm in x, y, or z translation or ±3 degrees pitch, roll or yaw). Table 1 shows characteristics for the participants included in this analysis. Associations of accuracy with other measures (Table 1) were in the expected direction though not significant ($p > 0.05$). Accuracy and response time of the sDSST were significantly correlated with score on the pencil and paper DSST test (Spearman ρ : 0.36, $p=0.03$ and 0.66, $p<0.0001$).

Spatial distribution of sDSST- related brain fMRI activation and relationship with accuracy

Brain peak activation while performing the sDSST was significantly greater than brain peak activation while performing the control condition (cluster probability (alpha) < 0.001) for ECF regions within the prefrontal cortex bilaterally and for left posterior parietal regions (BA 7,40) independent of group assignment and of atrophy index (not shown). Analyses to test the opposite direction of association (main effect of control condition > sDSST) were all not significant.

The correlation of fMRI signal with accuracy was positive and significant (Figure 2 and Table 2). For greater accuracy, the fMRI activation was significantly greater within ECF-related regions: left prefrontal cortex and right parietal cortex. Activation also extended caudally to the left sensori-motor cortex (pre- and post-central gyri) and left superior temporal gyrus. All analyses were independent of group assignment, sDSST response time and atrophy index. Analyses repeated using a voxel-wise and region-of-interest approach consistently showed similar results.

Relationship of fMRI activation, accuracy and connectivity abnormalities

Greater WMH volume and atrophy index were significantly associated with older age and lower score on the pencil and paper DSST (Table 1) Greater WMH was also associated with lower accuracy and longer response times on the sDSST. Association with atrophy index was in the expected direction though not statistically significant (Table 1). WMH volume was inversely correlated with the fMRI signal in ECF-related regions bilaterally (anterior cingulate cortex), as well as bilateral sensori-motor and right superior temporal gyrus (Figure 3 and Table 3). Atrophy index was not associated with fMRI brain activation during sDSST performance.

There was a significant and positive interaction (Figure 4 and Table 4) between accuracy and WMH volume within specific ECF-related (left posterior parietal).and non ECF- related regions (left sensori-motor regions). The association of WMH with fMRI activation varied as accuracy's values varied. Specifically, there was a positive correlation between WMH and fMRI signal as accuracy increased. In additional exploratory analyses within the group with WMH volume> median, greater accuracy was associated with greater bilateral activation in ECF regions (posterior parietal and cingulate cortex) and it extended to sensori-motor regions (not shown).

Discussion

The results of this functional neuroimaging study support the compensation model of cognitive aging in several ways. First, greater accuracy was associated with greater fMRI activation, mainly from ECF regions. Specifically, prefrontal cortices showed greater fMRI activation during sDSST performance with higher accuracy. Second, we found that higher WMH was associated with lower activation in regions that were also important for accuracy and that the accuracy-related networks seemed to partially overlap with the networks affected by higher WMH, mainly within the left hemisphere (compare the spatial distribution of the main effect of accuracy in Figure 2, with the main effect of WMH in Figure 3). While the negative correlation of WMH measure with accuracy was expected, the association of greater WMH with lower fMRI signal within the ECF-related regions (Figure 3) is a novel finding and it indicates that WMH may be an important determinant of patterns of brain functional activation and of behavioral response. These findings indicate that WMH may affect behavioral performance through reduction of activation within regions that are important to execute this task. Thirdly, there was a significant interaction between WMH and accuracy. The study of the spatial distribution of this interaction (Figure 4 and Table 4) indicates that there is an anterior to posterior progression and that the regions that showed interaction (Figure 4) only partially overlapped with the regions that showed a main effect of accuracy and a mani effect of WMH (Figures 2 and Figure 3). The significant interaction between WMH and accuracy within the left posterior parietal lobe suggests that this interference is focal and specific for ECF-networks that are not associated with WMH burden. The processes underlying this selected spatial distribution and antero-posterior shift will need to be further investigated. Taken as a whole, our findings indicate that for greater brain damage, the activation in regions important for accurately performing the DSST decreases, and activation in additional- extraneous- regions increases, specifically within regions that would not routinely be recruited to respond to this task and that are spared by the WMH degenerative process as observed in the main effect analyses. Thus, higher performance in older adults may be achieved through greater and more spread brain activation to counteract greater structural abnormalities or reduced “reserve”. The activation of non-ECF regions (eg. sensori-motor regions) to complete a ECF tasks may also indicate a less efficient or “non-functional” usage of neural activation and it is consistent with the notion of de-dedifferentiation in the older brain.(Baltes and Lindenberger 1997;Li 1999;Cabeza 2002) A potential additional pathway linking WMH with more diffuse activation is that increased WMH burden would lead to less activation in voxels associated with good performance at the group level and more spread to other voxels.

Importantly, in this study only some older adults with WMH above the median had greater performance and greater fMRI activation within the posterior parietal lobe. Future studies are needed to investigate the reasons why some older adults with WMH perform better than others. It is possible that the spatial distribution of WMH is more important than its total volume in impairing performance and brain activation. It is also possible that those with greater WMH volume and greater fMRI signal achieved greater performance because they had been exposed to other protective factors. For example, education and various lifestyle factors have been identified as surrogate markers of inherent neural resources. While the participants of this study completed a comprehensive lifestyle factors assessment, the exploratory sub-analyses of fMRI, structural images measure and behavioral performance for those within the intervention and control group yield very small numbers. The small number may impair the ability to examine group differences with adequate statistical power. Future studies examining indicators of brain reserve and the spatial distribution of structural integrity in large groups of older adults are warranted to elucidate the mechanisms underlying a sustained successful performance late in age. Other abnormalities in addition to those affecting brain connectivity, are neuronal metabolism and neurotransmission, which also need to be explored. In this fMRI study of aging we used standard registration methods and smoothing parameters, which is a potential

limitation as some have suggested that structural variability in older adults limits the registration, and can confound the interpretation of the fMRI results. One would expect this confound to lead to decreased activation in subjects with greater atrophy. In this study, we found no difference in activation that correlated atrophy index, thus we suspect that our results are not confounded by differences in brain registration. Other limitations in the study include that we have used a standard HRF for the fMRI analysis, whereas it is possible that the characteristic of the HRF are altered with age.

Acknowledgments

The authors thank P. Vincent, P. Kost, P. Varlashkin and S. Urda, for assistance in obtaining the data necessary for this analysis. Supported in part by Intramural Research Program, National Institute of Aging (NIA 263-MA-706016).

References

Baltes PB, Lindenberger U. Emergence of a powerful connection between sensory and cognitive functions across the adult life span: a new window to the study of cognitive aging? Psychol Aging 1997;12(1): 12–21. [PubMed: 9100264]

Brassen S, Büchel C, Weber-Fahr W, Lehmbeck JT, Sommer T, Braus DF. Structure-function interactions of correct retrieval in healthy elderly women. Neurobiol Aging 2009;30(7):1147–1156. [PubMed: 18023505]

Cabeza R. Hemispheric asymmetry reduction in older adults: the HAROLD model. Psychol Aging 2002;17(1):85–100. [PubMed: 11931290]

Cabeza R, Anderson ND, et al. Aging gracefully: compensatory brain activity in high-performing older adults. Neuroimage 2002;17(3):1394–1402. [PubMed: 12414279]

Cabeza R, Daselaar SM, et al. Task-independent and task-specific age effects on brain activity during working memory, visual attention and episodic retrieval. Cereb Cortex 2004;14(4):364–375. [PubMed: 15028641]

Calautti C, Serrati C, et al. Effects of age on brain activation during auditory-cued thumb-to-index opposition: A positron emission tomography study. Stroke 2001;32(1):139–146. [PubMed: 11136929]

Cox RW. AFNI: software for analysis and visualization of functional magnetic resonance neuroimages. Comput Biomed Res 1996;29(3):162–173. [PubMed: 8812068]

Friston K. Statistical parametric maps in functional imaging: A general linesr approach. Hum Brain Mapp 1995;2:189–210.

Grady CL. Effect of task difficulty on cerebral blood flow during perceptual matching for faces. Hum Brain Mapp 1996;4:227–239.

Grady CL. Introduction to the special section on aging, cognition, and neuroimaging. Psychol Aging 2002;17(1):3–6. [PubMed: 11931286]

Gunning-Dixon FM, Raz N. The cognitive correlates of white matter abnormalities in normal aging: a quantitative review. Neuropsychology 2000;14(2):224–232. [PubMed: 10791862]

Heuninckx S, Wenderoth N, et al. Neural basis of aging: the penetration of cognition into action control. J Neurosci 2005;25(29):6787–6796. [PubMed: 16033888]

Langenecker SA, Nielson KA, et al. fMRI of healthy older adults during Stroop interference. Neuroimage 2004;21(1):192–200. [PubMed: 14741656]

Li S. Cross-level unification: a computational exploration of the link between deterioration of neurotransmitter systems dedifferentiation of cognitive abilities in old age. Cognitive neuroscience of memory 1999:103–146.

Maldjian JA, Laurienti PJ, et al. An automated method for neuroanatomic and cytoarchitectonic atlas-based interrogation of fMRI data sets. Neuroimage 2003;19(3):1233–1239. [PubMed: 12880848]

Matarazzo JD, Herman DO. Base rate data for the WAIS-R: test-retest stability and VIQ-PIQ differences. J Clin Neuropsychol 1984;6(4):351–366. [PubMed: 6501578]

Mattay VS, Fera F, et al. Neurophysiological correlates of age-related changes in human motor function. Neurology 2002;58(4):630–635. [PubMed: 11865144]

McIntosh AR, Sekuler AB, et al. Recruitment of unique neural systems to support visual memory in normal aging. Curr Biol 1999;9(21):1275–1278. [PubMed: 10556091]

Nordahl CW, Ranganath Charan, Yonelinas Andrew P, DeCarli Charles, Fletcher Evan, Jagust William J. White Matter Changes Compromise Prefrontal Cortex Function in Healthy Elderly Individuals. Journal of Cognitive Neuroscience 2006;18(3):418–429. [PubMed: 16513006]

Pahor M, Blair SN, et al. Effects of a physical activity intervention on measures of physical performance: Results of the lifestyle interventions and independence for Elders Pilot (LIFE-P) study. J Gerontol A Biol Sci Med Sci 2006;61(11):1157–1165. [PubMed: 17167156]

Park DC, Reuter-Lorenz P. The adaptive brain: aging and neurocognitive scaffolding. Annu Rev Psychol 2009;60:173–196. [PubMed: 19035823]

Persson J, Nyberg L, Lind J, Larsson A, Nilsson LG, Ingvar M, Buckner RL. Structure-function correlates of cognitive decline in aging. Cereb Cortex 2006;16(7):907–915. [PubMed: 16162855]

Persson J, Nyberg L. Altered brain activity in healthy seniors: what does it mean? Prog Brain Res 2006;157:45–56. [PubMed: 17167903]

Persson J, Sylvester CY, et al. Selection requirements during verb generation: differential recruitment in older and younger adults. Neuroimage 2004;23(4):1382–1390. [PubMed: 15589102]

Reuter-Lorenz PA. Neural recruitment and cognitive aging: two hemispheres ar ebetter than one especially as you age. Psychol Sci 1999;10:494–500.

Reuter-Lorenz PA. Neurocognitive again of storage and executive processes. Eur. J Cogn. Psychol 2001;13:257–258.

Reuter-Lorenz PA, Jonides J, et al. Age differences in the frontal lateralization of verbal and spatial working memory revealed by PET. J Cogn Neurosci 2000;12(1):174–187. [PubMed: 10769314]

Reuter-Lorenz PA, Lustig C. Brain aging: reorganizing discoveries about the aging mind. Curr Opin Neurobiol 2005;15(2):245–251. [PubMed: 15831410]

Rosano C, Aizenstein H, et al. Functional neuroimaging indicators of successful executive control in the oldest old. Neuroimage 2005;28(4):881–889. [PubMed: 16226041]

Rosano C, Becker J, et al. Morphometric analysis of gray matter volume in demented older adults: exploratory analysis of the cardiovascular health study brain MRI database. Neuroepidemiology 2005;24(4):221–229. [PubMed: 15832060]

Rosano C, Newman AB, et al. Association between lower digit symbol substitution test score and slower gait and greater risk of mortality and of developing incident disability in well-functioning older adults. J Am Geriatr Soc 2008;56(9):1618–1625. [PubMed: 18691275]

Rypma B. Age-related changes in brain-behavior relationships: eveidence from event-related functional MRI studies. Eur. J Cogn. Psychol 2001;13:235–256.

Rypma B, D'Esposito M. The roles of prefrontal brain regions in components of working memory: effects of memory load and individual differences. Proc Natl Acad Sci U S A 1999;96(11):6558–6563. [PubMed: 10339627]

Salthouse TA. The role of memory in the age decline in digit-symbol substitution performance. J Gerontol 1978;33(2):232–238. [PubMed: 637915]

Salthouse TA. How localized are age-related effects on neuropsychological measures. Neuropsychology 1996;10:272–285.

Udupa J. Fuzzy connectedness and object definiteion: theory, algorithms, and applications in image segmentation. Graphical Models and Image Processing 1996;58:246–261.

Ward NS, Frackowiak RS. Age-related changes in the neural correlates of motor performance. Brain 2003;126(Pt 4):873–888. [PubMed: 12615645]

Weschler Adult Intelligence Scale-Revised. San Antonio: T. P. C.; 1981.

West RL. An application of prefrontal cortex function theory to cognitive aging. Psychol Bull 1996;120 (2):272–292. [PubMed: 8831298]

Wu M, Carmichael O, et al. Quantitative comparison of AIR, SPM, and the fully deformable model for atlas-based segmentation of functional and structural MR images. Hum Brain Mapp 2006;27(9):747–754. [PubMed: 16463385]

Zandbelt BB, Gladwin TE, et al. Within-subject variation in BOLD-fMRI signal changes across repeated measurements: quantification and implications for sample size. Neuroimage 2008;42(1):196–206. [PubMed: 18538585]

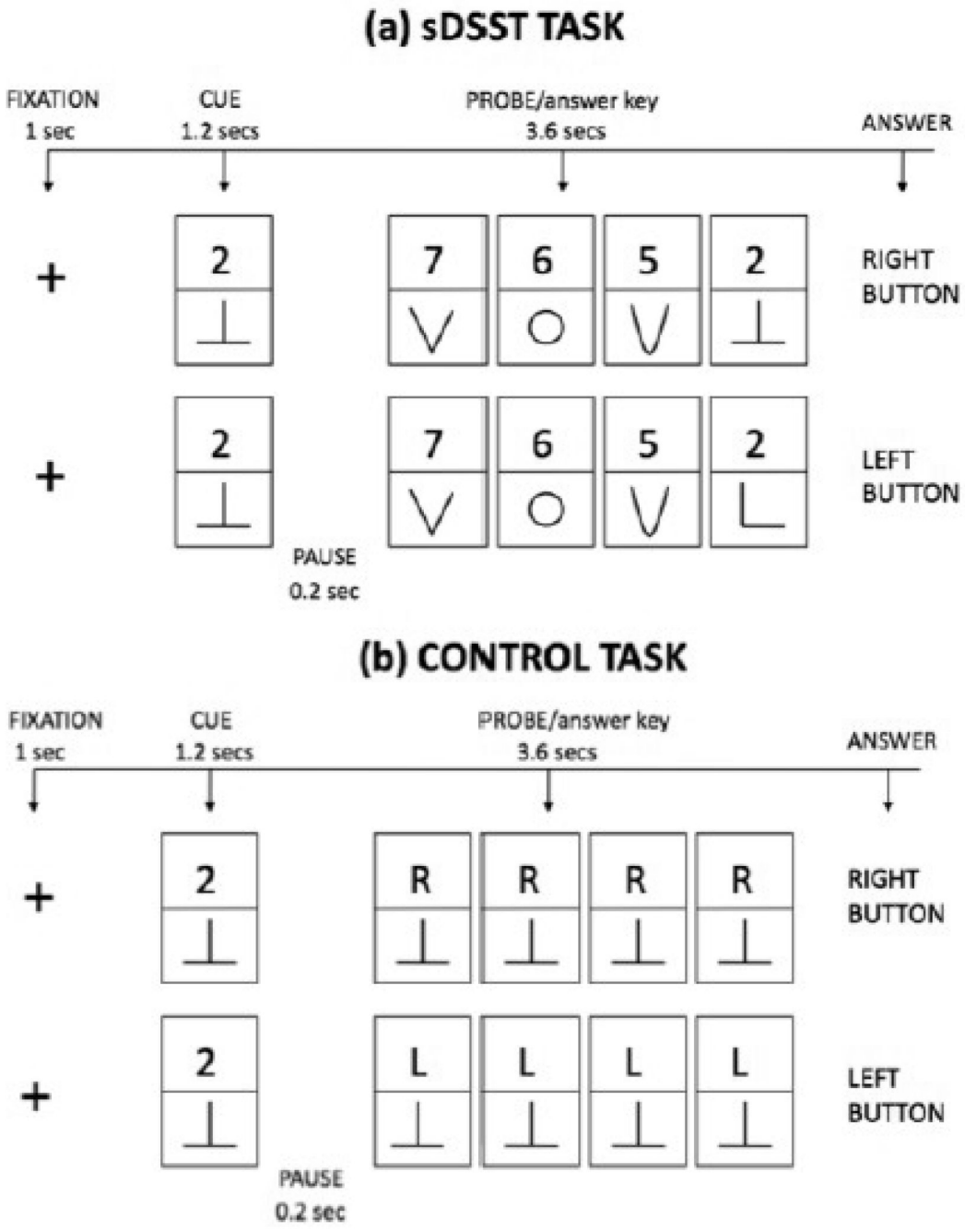

Figure 1. Schematic diagram illustrating (a) DSST and (b) control condition tasks

Schematic representation of the tasks that the participants were administered during the brain fMRI scanning session. Two examples are shown for the sDSST (matching right button and not matching left button) and for the control condition (right button and left button).

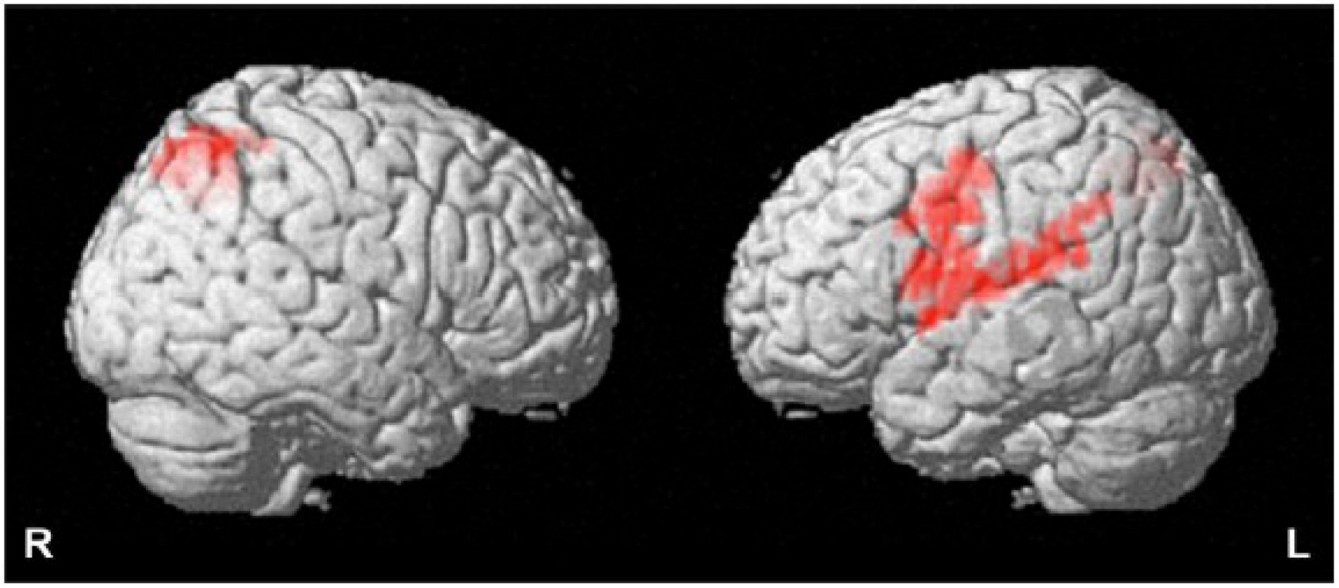

Figure 2. Spatial distribution of brain functional MRI activation that were positively correlated with accuracy during sDSST task performance

T maps of analysis of task-related activity positively correlated with accuracy during sDSST task performance. Adjusted for group assignment, atrophy index and sDSST response time. Threshold was at t= 1. 71 and cluster probability (alpha) < 0.001. See table 2 for list of regions.

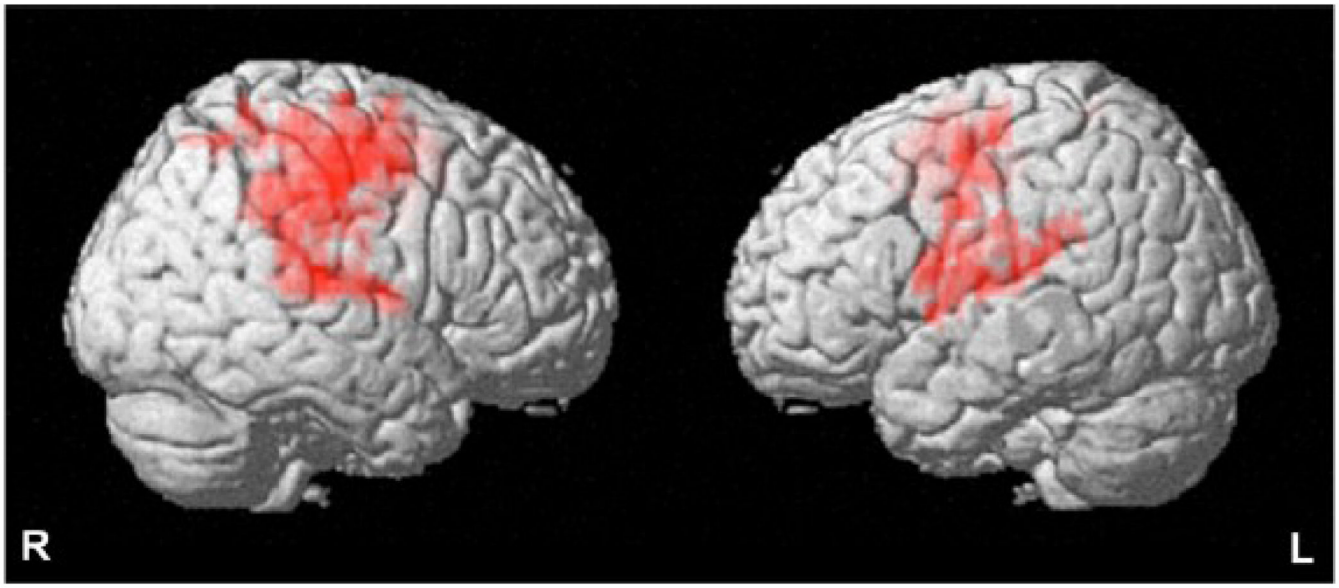

Figure 3. Spatial distribution of functional brain MRI activation showing negative correlation with WMH burden

T maps of analysis to identify the regions that showed negative correlation between WMH burden and functional MRI activation (sDSST > control condition) adjusted for atrophy index and group assignment. Threshold was at t= 1. 71 and cluster probability (alpha) < 0.001. See table.3 for list of regions.

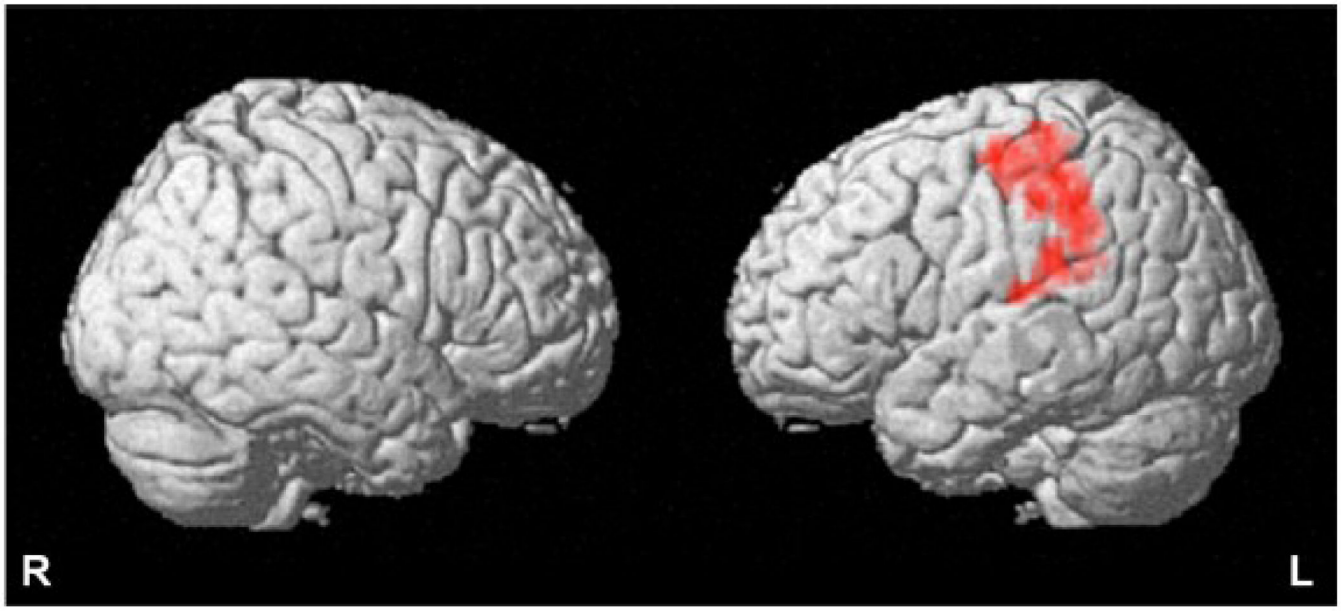

Figure 4. Spatial distribution of functional brain MRI activation showing positive interaction of WMH burden by accuracy during sDSST task

T maps of analysis to identify the regions that showed interaction of WMH volume by accuracy during sDSST task. Analyses were adjusted for group assignment, atrophy and sDSST response time. Threshold was at t= 1. 71 and cluster probability (alpha) < 0.001. See table 4 for list of regions.

Table 1

Participants' Characteristics (n=25)

Measure	Mean (SD)	Correlations with imaging makers of brain Structure Spearman ρ (p value)	
		Atrophy index[1]	WMH[2]
Age, Yrs,	81.67 (3.47)	0.58 (p=0.001)	0.61 (p <0.0001)
Minimental Score,	27.52 (1.9)	0.04 (p=0.4)	−0.26 (p=0.09)
Pencil and Paper DSST, correct points,	53.48 (17.12)	−0.48 (p=0.005)	−0.49 (p=0.004)
sDSST Accuracy, %	0.90 (0.13)	−0.17 (p=0.02)	−0.77 (p<0.0001)
sDSST response time, msecs	1640.56 (314.87)	0.29 (p=0.07)	0.62 (p<0.0001)
IMAGING MAKERS OF BRAIN STRUCTURE			
Atrophy index[1]	0.72 (0.08)	-	0.16 (p=0.2)
WMH[2]	0.50 (0.61)	0.16 (p=0.2)	-

[1] Atrophy index: (Gray Matter volume/cerebrospinal fluid volume)$^{-1}$

[2] White Matter Hyperintensities Measure (WMH): WMH voxel count divided by sum of gray matter and white matter voxel counts.

Table 2

Spatial distribution of correlation of accuracy with brain functional MRI activation during sDSST task performance

This table reports the spatial distribution of the association of accuracy with the mean group activation (obtained from the sDSST > control condition contrast), including the size of cluster, the maximum Z statistic for the cluster and the location of the maximum Z statistic in Talairach coordinates. The analyses were adjusted for group assignment, atrophy index and sDSST response time. The corrected alpha is the probability of a false positive detection based on the combination of individual voxel probability thresholding and minimum cluster size thresholding.

Regions	Cluster Size	Peak Z-Score	Talairach Coordinate for Peak Z-Score
Regions positively correlated with accuracy during sDSST performance			
Left prefrontal cortex	968	3.25	−45.54, −8.17, 30.8[1]
Right posterior parietal cortex	451	2.84	35.64, −53.56, 55.18[2]
Regions negatively correlated with accuracy during sDSST performance			
No significant voxels			

[1] This cluster had its peak in the left precentral gyrus (BA 6) extended to middle and prefrontal gyri (BA 4, 9, 44), and covered postcentral gyrus (BA 40, 43) and superior temporal gyrus (BA 42).

[2] This cluster had its peak in the right superior parietal lobule medially (BA 7) and extended to the inferior parietal lobule (BA 40).

Table 3

Spatial distribution of correlation of WMH volume with brain functional MRI activation during sDSST task performance

Regions that show correlation between the structural measure (WMH measure) and task (sDSST > control condition) adjusted for atrophy index and group assignment, including the size of cluster, the maximum Z statistic for the cluster and the location of the maximum Z statistic in Talairach coordinates. The corrected alpha is the probability of a false positive detection based on the combination of individual voxel probability thresholding and minimum cluster size thresholding.

Regions	Cluster Size	Peak Z-Score	Talairach Coordinate for Peak Z-Score
Regions Negatively Correlated with WMH burden			
Left anterior cingulate cortex	524	4.05	−3.96, −1.25, 52.56[1]
Right anterior cingulate cortex	561	3.95	19.8, −17.58, 36.8[2]
Left prefrontal cortex	885	4.19	−23.76, −7.61, 41.83[3]
Right prefrontal cortex	1976	4.63	29.7, −9.55, 41.93[4]
Regions positively correlated with WMH burden			
No significant voxels			

[1] This cluster had its peak in the left medial frontal gyrus (BA 6) covered the cingulate gyrus (BA 24, 32) and superior frontal gyrus (BA 6).

[2] This cluster had its peak in the right cingulate gyrus (BA 24, 32) extended to medial frontal gyrus and superior frontal gyrus (BA 6).

[3] This cluster had its peak in the left middle frontal gyrus and covered the sensori-motor cortex (pre- and post-central gyri: BA 3, 40, 43, 44).

[4] This cluster had its peak in the right middle frontal gyrus (BA 6) covered the sensori-motor cortex (pre- and post-central gyri: BA 3, 4, 6, 40, 43, 44), superior frontal gyrus (BA 6) and superior temporal gyrus (BA 42).

Table 4

Spatial distribution of functional brain MRI activation showing significant interaction of WMH burden by accuracy during sDSST task

This table reports the regions that showed interaction of WMH volume by accuracy during the sDSST task, including the size of cluster, the maximum Z statistic for the cluster and the location of the maximum Z statistic in Talairach coordinates. Analyses were adjusted for group assignment, atrophy index and sDSST response time. The corrected alpha is the probability of a false positive detection based on the combination of individual voxel probability thresholding and minimum cluster size thresholding.

Regions	Cluster Size	Peak Z-Score	Talairach Coordinate for Peak Z-Score
Regions with positive interaction term (Accuracy by WMH)			
Left posterior parietal cortex	777	3.08	−37.62, −27.96, 62.19[1]
Regions with negative interaction term (Accuracy by WMH)			
No significant voxels			

[1] This cluster had its peak in the left postcentral gyrus (BA 3), it covered the inferior parietal lobule (BA 40) and sensori-motor cortex (pre-post-central gyri : BA 2, 3 and 4).